NASA Investigation of a Claimed "Overlap" Between Two Gust Response Analysis Methods

Boyd Perry III*
NASA Langley Research Center, Hampton, Virginia 23665-5225
and
Anthony S. Pototzky† and Jessica A. Woods‡
Planning Research Corporation, Hampton, Virginia

This paper presents the results of a NASA investigation of a claimed "overlap" between two gust response analysis methods: the statistical discrete gust (SDG) method and the power spectral density (PSD) method. The claim is that the ratio of an SDG response to the corresponding PSD response is 10.4. Analytical results presented in this paper for several different airplanes at several different flight conditions indicate that such an overlap does appear to exist. However, the claim was not met precisely: a scatter of up to about 10% about the 10.4 factor can be expected.

Introduction

THE U.S. Federal Aviation Administration (FAA) has formed an ad hoc international committee of gust specialists, which draws its membership from domestic and foreign civil airworthiness authorities, airframe manufacturers, and research laboratories. The committee's work is part of an ongoing effort to rationalize and improve the gust criteria applied by U.S. and European airworthiness authorities. The effort includes the investigation of candidate analysis methods for gust-loads certification.

The statistical discrete gust (SDG) method of computing gust loads[1] was identified by the ad hoc committee as a candidate for further investigation because of a feature that makes the SDG method very attractive: its ability to compute 1) maximized and time-correlated gust loads and 2) the gust profiles that produce these loads. Time correlation provides knowledge of the values (magnitudes and signs) of all loads when one particular load has attained its maximum (positive or negative) value. If the particular maximum load is critical for design, then an airplane manufacturer may employ the SDG method to obtain a set of design loads to physically apply to a test specimen. This is not possible with the more familiar power spectral density (PSD) method.

J. G. Jones of the Royal Aerospace Establishment, Farnborough, United Kingdom, is the developer of the SDG method. Jones claims[2] that under certain circumstances the SDG and PSD methods produce essentially the same numerical results, or that "...the former is essentially simply an approximate numerical implementation of the latter." Jones refers to this situation as the SDG-PSD "overlap."

In response to a recommendation from the ad hoc committee, in the fall of 1986, the FAA requested assistance from NASA to investigate Jones' claim of an SDG-PSD overlap. Over the course of the following 24 months, NASA performed the requested investigation, and the purpose of this paper is to report the results of that investigation.

Scope of NASA Investigation

This investigation is limited to linear systems. It is recognized that the ultimate usefulness of a candidate gust-loads analysis method depends on the ability of that method to include and correctly account for nonlinearities in the aerodynamics, structure, and control systems. The usefulness of the SDG method with regard to such nonlinearities is currently being debated[3] but is beyond the scope of the present investigation.

Descriptions of Analysis Methods

Both the SDG method and the PSD method compute the response of an airplane to atmospheric turbulence. The former is performed in the time domain, the latter in the frequency domain. The input to both methods is the same numerical description of the airplane. This section of the paper provides a heuristic outline of each method.

Statistical Discrete Gust Method

The objective of the SDG method is to determine analytically the maximum, or worst-case, responses of an airplane to discrete gusts representative of atmospheric turbulence. The method is carried out in the time domain through the calculation of response time histories. The method was originally developed more than 15 years ago by Jones,[1] and over the

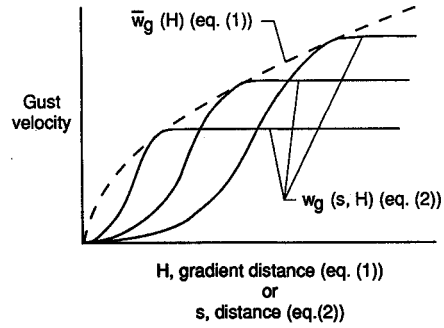

Fig. 1 Family of equiprobable smoothly varying ramp-hold gusts for SDG method.

Received March 25, 1989; presented as Paper 89-1376 at the AIAA 30th Structures, Structural Dynamics and Materials Conference, Mobile, AL, April 3-5, 1989; revision received Jan. 12, 1990.

*Aerospace Engineer.
†Engineering Specialist, Aerospace Technologies Division; currently at Lockheed Engineering and Sciences Company, Hampton, VA. Member AIAA.
‡Structures Engineer, Aerospace Technologies Division; currently at NASA Langley Research Center, Hampton, VA. Member AIAA.

course of those years, and continuing into the present, the method has undergone refinements and improvements.[2,4-7]

The SDG method is based on the assumption that atmospheric turbulence is comprised of a family of discrete equiprobable, smoothly varying, ramp-hold gusts, whose maximum magnitudes w_g vary as indicated by the dashed envelope in Fig. 1 and as defined by the following equation

$$\bar{w}_g(H) = U_0 H^k \qquad \text{for } 0 \le H \le L \tag{1}$$

where U_0 is a gust-intensity parameter, H the gradient distance, k the fractional exponent, and L the scale of turbulence.

Each discrete gust is defined by a transient portion (the first half of a one-minus-cosine wave) followed by a steady-state portion (whose value is equal to the value of the transient portion at the end of the transient). The length of the transient is the gradient distance. The expression for one member of the family of gusts is

$$w_g(s,H) = \begin{cases} \dfrac{\bar{w}_g(H)}{2}\left[1-\cos\left(\dfrac{\pi s}{H}\right)\right] & \text{for } 0 \le s \le H \\ \bar{w}_g(H) & \text{for } H < s \le L \end{cases} \tag{2}$$

where s is distance and is related to time through the velocity V.

In the implementation of the method, an airplane is subjected to the following inputs, applied one at a time: 1) all possible single gusts, 2) all possible combinations of two gusts with all possible "spacings" (defined later) between the gusts, 3) all possible combinations of three gusts with all possible combinations of spacing between the gusts, and ... n) all possible combinations of n gusts with all possible combinations of spacing between the gusts.

In general, time histories of each airplane response quantity due to each of the (extremely large number of) inputs is examined to find the worst-case response (that is, the largest positive or negative peak value) of each response quantity. The combination of gusts that produces the worst-case response is referred to as the critical gust pattern.

Figure 2 contains a sketch of a combination of three gusts, labeled 1, 2, and 3, in the time domain. Quantities τ_1 and τ_2 in the figure represent spacings in time between the completion of the transient of one gust and the start of the transient of the next. As indicated in the figure by the direction of the arrows, τ_1 and τ_2 are positive; however, τ_1 and τ_2 may also be negative. When either τ_1 or τ_2 is negative, the associated gusts are said to overlap one another.

For an airplane modeled as a linear system, this extremely large number of inputs may be reduced to a manageable number by taking advantage of superposition, as described in Ref. 4. With superposition, worst-case response to combinations of two or more gusts are determined by the responses to single gusts only.

As the number of gusts in a combination increases from 1 to n, the probability of encountering that combination in the assumed atmospheric turbulence decreases, and this decrease in probability is accounted for analytically through the use of amplitude reduction factors. The amplitude reduction factors reduce the magnitudes of the inputs (and for a linear system, reduce the magnitudes of the responses by the same ratio), thereby bringing the responses to all single gusts and the responses to all combinations of gusts to the same level of probability of occurrence.

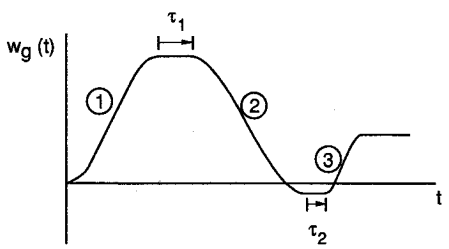

Fig. 2 Combination of three single gusts.

The following equation illustrates how the overall worst-case response is determined.

$$\bar{\gamma} = \max\begin{cases} p_1\gamma_1 \\ p_2\gamma_2 \\ p_3\gamma_3 \\ p_4\gamma_4 \\ \vdots \\ p_n\gamma_n \end{cases} \tag{3}$$

The γ_i are the individual worst-case responses to a combination of i gusts; the p_i are the corresponding amplitude reduction factors. The overall worst-case response $\bar{\gamma}$ is the worst of the worst or the maximum of the products of the sums of the γ_i and their corresponding p_i. The critical gust pattern is constructed by summing single ramp inputs associated with $\bar{\gamma}$.

Two implementations of the SDG method will be addressed in this paper. Jones refers to these implementations as "method 1" and "method 2." Method 1 contains simplifying assumptions about the characteristics of critical gust patterns and approximations in the computation of the amplitude reduction factors that make it computationally faster, but more restrictive and less exact than method 2. Method 2 is more general and for this reason it will be discussed first.

Method 2

In method 2, there are no restrictions concerning the characteristics of the critical gust patterns. Critical gust patterns are comprised of single gusts whose magnitudes may be negative or positive (representing either up or down gusts) in any order and whose spacing in time may be negative or positive (representing subsequent gusts that either do or do not overlap each other).

The amplitude reduction factors are computed based on the following formula[7]

$$p_1 = 1 \tag{4a}$$

$$p_i = \frac{1}{0.88\sqrt{I_i/I_1}} \qquad \text{for } i \ge 2 \tag{4b}$$

where

$$I_i = \int_0^{s_i} \left(\frac{d^{5/6}v(s)}{ds^{5/6}}\right)^2 ds \tag{5}$$

and where $v(s)$ is a gust pattern made up of i individual ramps, s is distance, and s_i is the distance at the completion of the transient of the ith ramp. Numerical evaluation of the fractional derivative in Eq. (5) is outlined in the appendix of Ref. 6.

Method 1

In method 1, there are restrictions concerning the characteristics of the critical gust patterns. Critical gust patterns are comprised of single gusts whose magnitudes must have alternating negative and positive signs (representing alternating up and down gusts) and whose spacing in time must be positive (representing subsequent gusts that do not overlap each other).

In method 1, the amplitude reduction factors are computed based on the following formula[7]

$$p_1 = 1 \tag{6a}$$

$$p_i = \frac{1}{0.88\sqrt{i}} \qquad \text{for } i \ge 2 \tag{6b}$$

which is an approximation to Eq. (4). For a gust pattern that satisfies the method 1 restrictions, the radical in Eq. (4) consistently reduces to the radical in Eq. (6), and the method 2 results are almost identical to those of method 1.

Power Spectral Density Method

The PSD method was first applied to the airplane turbulence response problem 40 years ago.[8] Since that time the PSD method has become so widely accepted that the federal aviation regulations [specifically, FAR 25.305(d)] require that, unless a more rational method is used, an airplane manufacturer must use the PSD method to establish the dynamic response of its airplanes to atmospheric turbulence.

The fundamental quantity of the PSD method is the PSD function, or power spectrum. A power spectrum contains all of the statistical information describing a random process, including the root-mean-square (rms) value. The random processes in question in the present application are atmospheric turbulence (the input random process) and airplane responses (the output random processes). The input is assumed Gaussian, and because the system is assumed linear, the output is also Gaussian. It is assumed that the turbulence is one-dimensional (that is, uniform across the span), homogeneous, isotropic, and "frozen" in space during the time it takes the airplane to traverse its own length.

The input and output PSD functions are related to each other through the square of the modulus of the airplane frequency response function, as given by the following equation

$$\Phi_y(\omega) = \Phi_{w_g}(\omega)\,|H_y(i\omega)|^2 \tag{7}$$

where $\Phi_y(\omega)$ is the airplane response power spectrum and $\Phi_{w_g}(\omega)$ is the atmospheric turbulence power spectrum. The airplane frequency response function $H_y(i\omega)$ represents the response (magnitude and phase), over a range of frequencies, of quantity y to a unit sinusoidal gust velocity. $H_y(i\omega)$ contains all the dynamics of the airplane (rigid-body modes and elastic modes).

For present purposes, the von Kármán form of $\Phi_{w_g}(\omega)$ was chosen and is given by the following equation[9]

$$\Phi_{w_g}(\omega) = \frac{\sigma_{w_g}^2 L}{\pi V}\,\frac{1+(8/3)\left[1.339(L/V)\omega\right]^2}{\left\{1+\left[1.339(L/V)\omega\right]^2\right\}^{11/6}} \tag{8}$$

Figure 3 contains a log-log plot of $\Phi_{w_g}(\omega)$ as a function of ω. For illustration purposes the quantity $\sigma_{w_g}^2$ and the ratio L/V were chosen to be unity. At low values of frequency, the function asymptotically approaches a constant value $(\sigma_{w_g}^2 L/\pi V)$; at high values of frequency, the function asymptotically approaches zero as $\omega^{-5/3}$. At intermediate values of frequency, the function makes a transition between the low- and high-frequency asymptotes and reaches a maximum, referred to as the "knee." The corresponding frequency is referred to as the "knee frequency," ω_{knee}, where

$$\omega_{\text{knee}} = 0.457(V/L) \tag{9}$$

The rms values of random processes w_g and y may be obtained by performing the following operations

$$\sigma_{w_g} = \left[\int_0^\infty \Phi_{w_g}(\omega)\,d\omega\right]^{1/2} \tag{10}$$

and

$$\sigma_y = \left[\int_0^\infty \Phi_y(\omega)\,d\omega\right]^{1/2} \tag{11}$$

$\bar{A}$ is the normalized response quantity, defined as the ratio of the rms of the output to the rms of the input

$$\bar{A} = \sigma_y/\sigma_{w_g} \tag{12}$$

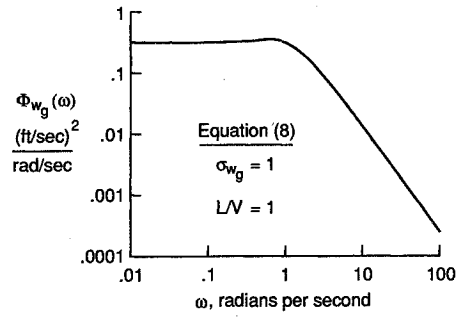

Fig. 3 Von Kármán PSD function.

Table 1 Conditions for the statistical discrete gust-power spectral density overlap

SDG quantities [Refer to Eqs. (1) and (2)]	PSD quantities [Refer to Eqs. (8) and (9)]
$k = 1/3$	von Kármán form of $\Phi_{w_g}(\omega)$
$U_0 = 1$ fps	$\sigma_{w_g} = 1$ fps
$L = 2500$ ft	$L = 2500$ ft
—	$\omega_{sp} \gg \omega_{knee}$

Definition of the SDG-PSD Overlap

Jones claims that under certain circumstances the SDG and PSD methods produce essentially the same numerical results,[2] and he refers to this situation as the SDG-PSD overlap. The quantitative definition of the overlap is given by the following equation

$$\bar{\gamma} = 10.4\bar{A} \tag{13}$$

where $\bar{\gamma}$ is defined by Eq. (3) and $\bar{A}$ is defined by Eq. (12). The relationship in Eq. (13) implies that design loads are proportional to $\bar{A}$, which is consistent with the design envelope gust loads criterion.[10]

The circumstances under which Eq. (13) is valid are summarized in Table 1. Quantities from the SDG method are found in Eqs. (1) and (2) and quantities from the PSD method, in Eqs. (8) and (9). The value 1/3 for exponent k in Eq. (1) corresponds to the $-5/3$ high-frequency asymptote of the von Kármán power spectrum in Eq. (8). For both the SDG and PSD methods, unit gust velocities and the standard value of scale of turbulence are used. In addition, there is a requirement that the airplane under investigation be described by linear equations and that the frequency of the short-period mode be much greater than the knee frequency of the von Kármán power spectrum. With these conditions met, Jones claims that the 10.4 factor of Eq. (13) will be obtained if SDG and PSD analyses are performed for the same vehicle.

Approach for Verification of the Overlap

The approach taken in the NASA investigation of the SDG-PSD overlap was to perform SDG and PSD analyses for several airplanes at different flight conditions and to compare the corresponding responses from each method to see if the 10.4 factor was obtained. To maintain impartiality and independence during the investigation, NASA wrote its own computer codes and chose its own configurations, flight conditions, and response quantities. In an attempt to define quantitatively the limits of the overlap, several parameters were varied.

Both rigid-body analyses and fully flexible analyses were performed: rigid-body analyses using method 1 only for five configurations and fully flexible analyses using methods 1 and 2 for one configuration. All were symmetric longitudinal analyses with the vertical component of atmospheric turbulence as the disturbance quantity.

Table 2 Example configurations for rigid-body analyses

Configuration number	Vehicle	Flight condition		Short period frequency, ω_{sp}, rad/s	$\frac{\omega_{sp}}{\omega_{knee}}$
		Mach no.	Altitude, ft		
1	NASA DAST ARW-2 (Firebee II drone)	0.70	15,000	3.44	28.8
2	Etkin example transport	0.74	30,000	1.44	10.8
3	OMAC laser 300	0.33	Sea level	3.87	58.2
4	Sabreliner (without active controls)	0.50	20,000	2.14	22.6
5	Sabreliner (with active controls)	0.50	20,000	1.89	19.9

Table 3 Summary of statistical discrete gust (method 1) and power spectral density results for rigid-body analyses

Configuration number	Response quantity (units)	PSD result	SDG results				
		$\bar{A}$ (units)/fps	Critical gust pattern			$\bar{\gamma}$ (units)	$\frac{\bar{\gamma}}{\bar{A}}$
			n	Overlap	Direction		
1	Pitch rate, $\dot{\theta}$ (rad/s)	0.002062	2	No	Opp.	0.02172	10.53
	c.g. vert. accel., Δn (g)	0.02827	2	No	Opp.	0.3041	10.76
2	Pitch rate, $\dot{\theta}$ (rad/s)	0.0006212	1	n/a	n/a	0.006913	11.13
	c.g. vert. accel., Δn (g)	0.01546	1	n/a	n/a	0.1511	9.77
3	Pitch rate, $\dot{\theta}$ (rad/s)	0.005368	1	n/a	n/a	0.05579	10.39
	c.g. vert. accel., Δn (g)	0.02412	2	No	Opp.	0.2584	10.71
4	Pitch rate, $\dot{\theta}$ (rad/s)	0.001151	1	n/a	n/a	0.01231	10.69
	c.g. vert. accel., Δn (g)	0.01936	1	n/a	n/a	0.1842	9.51
5	Pitch rate, $\dot{\theta}$ (rad/s)	0.0008433	1	n/a	n/a	0.009133	10.83
	c.g. vert. accel., Δn (g)	0.01994	1	n/a	n/a	0.1947	9.77
	Control surf. defl., δ (rad)	0.0003686	1	n/a	n/a	0.003573	9.69

Mean: 10.32; standard deviation: 0.56.

Rigid-Body Analyses

For the rigid-body analyses, the short-period approximation to the longitudinal small-perturbation equations of motion[11] were used. These equations are written in stability axes and employ stability derivatives to approximate the effects of unsteady aerodynamics. Response quantities for these analyses include pitch rate, vertical acceleration at the vehicle center of gravity, and control surface deflection.

Fully Flexible Analyses

For the fully flexible analyses, the equations of motion of a flexible vehicle were used. Aerodynamic characteristics were determined by a doublet-lattice, unsteady aerodynamics code.[12] The equations of motion are derived through a modal approach using Lagrange's equations resulting in linearized small-perturbation matrix equations of the form

$$[M]\{\ddot{q}\} + [D]\{\dot{q}\} + [K]\{q\} + \tfrac{1}{2}\rho V^2[Q]\{q\} = \tfrac{1}{2}\rho V^2\{Q_g\}w_g \tag{14}$$

where M, D, and K are, respectively, the generalized mass, damping, and stiffness matrices, Q and Q_g are the generalized aerodynamic force matrices due to vehicle motion and gust, q is the vector of generalized coordinates, ρ the fluid density, V the velocity, and w_g the gust velocity.

Response quantities included angular rates and linear accelerations, shear forces, bending moments, and torsion moments at several locations on the example configuration. The rates and accelerations are obtained by weighting the generalized-coordinate rates and accelerations by modal slopes and deflections. The forces and moments are obtained by the summation of forces method of computing dynamic loads.[13]

Numerical Results

Unless specifically identified as being otherwise, all numerical results presented in this section of the paper meet the conditions of SDG-PSD overlap as defined in Table 1.

Rigid-Body Results

In performing the rigid-body analyses, five different configurations, spanning a wide range of vehicle types, weights, and flight conditions, were used. Table 2 summarizes the characteristics of these configurations.

For each configuration, the PSD method and method 1 of the SDG method were performed using the short-period approximation to the equations of motion. For the PSD method, 250 points were used in the numerical integration of Eqs. (10)

Table 4 Summary of statistical discrete gust (method 2) and power spectral density results for fully flexible analyses

Response quantity (units)	PSD result $\bar{A}$ (units)/fps	SDG results: Critical gust pattern n	Overlap	Direction	$\bar{\gamma}$ (units)	$\bar{\gamma}/\bar{A}$
Outboard shear force (lb)	0.6223	4	Yes	Same	6.400	10.28
Outboard bending moment (ft lb)	0.2153	3	No	Opp.	2.385	11.08
Outboard torsion moment (ft lb)	0.2366	3	No	Opp.	2.720	11.50
Mid shear force (lb)	8.428	3	Yes	Same	94.82	11.25
Mid bending moment (ft lb)	19.41	3	Yes	Same	212.7	10.96
Mid torsion moment (ft lb)	2.657	4	Yes	Same	28.54	10.74
Pitch rate, c.g. (rad/s)	0.009581	5	No	Opp.	0.1015	10.59
Vertical acceleration, c.g. (fps^2)	3.515	10	Yes	Same	29.85	8.49
Vertical acceleration, span sta. 82 in. (fps^2)	156.6	4	No	Opp.	1478.0	9.44
Vertical acceleration, span sta. 84 in. (fps^2)	191.7	4	No	Opp.	1941.0	10.13

DAST ARW-2 Mach number = 0.7; altitude = 15,000 ft; $\omega_{sp}/\omega_{knee} = 21.7$. Mean: 10.45; standard deviation: 0.91.

and (11). For the SDG method, the vehicles were each subjected to about 50 single ramps. Table 3 summarizes these results. As indicated in the table, all critical gust patterns were comprised of either one ($n=1$) or two ($n=2$) single gusts. None of the $n=2$ cases had either overlapping gusts in the critical pattern or subsequent gusts in the same direction. Thus, the characteristics of the critical gust patterns for all cases comply with the restrictions that apply to method 1.

In the last column of the table, it is seen that all ratios of $\bar{\gamma}/\bar{A}$ fall between 9.51 (8.6% below 10.4) and 11.13 (7% above 10.4). The mean value of the ratios is 10.32 with a standard deviation of 0.56.

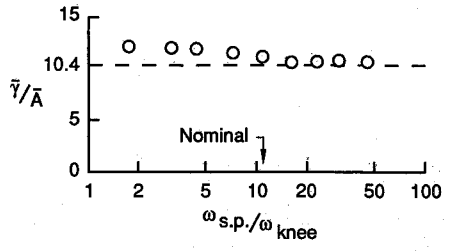

Fig. 4 Comparisons of SDG (method 1) and PSD results for rigid-body analyses as a function of frequency ratio; configuration 2, pitch-rate response.

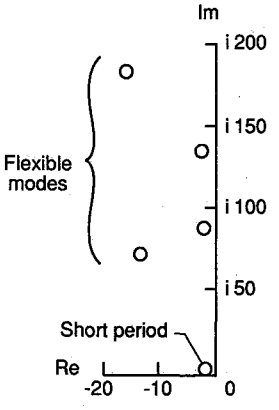

Fig. 5 Eigenvalues of DAST ARW-2 configuration; Mach number 0.7, altitude 15,000 ft.

Variation of the $\omega_{sp}/\omega_{knee}$ Ratio

An investigation was performed to determine the effect of the $\omega_{sp}/\omega_{knee}$ ratio on the resulting $\bar{\gamma}/\bar{A}$ ratios. Using configuration 2, the value of C_{m_α} was artificially varied to vary the short-period frequency, and the SDG and PSD analyses were reperformed. Eight additional values of C_{m_α} were chosen, four above and four below the nominal value, resulting in about a factor-of-five reduction and a factor-of-five increase in short-period frequency. Results of this investigation are presented in Fig. 4.

Figure 4 contains a semilog plot of the $\bar{\gamma}/\bar{A}$ ratio for pitch-rate response as a function of the $\omega_{sp}/\omega_{knee}$ ratio for configuration 2. At values of the $\omega_{sp}/\omega_{knee}$ ratio below 10 the $\bar{\gamma}/\bar{A}$ ratios depart by almost 20% from 10.4; at values of the $\omega_{sp}/\omega_{knee}$ ratio above 10, the $\bar{\gamma}/\bar{A}$ ratios remain very close to 10.4. These results indicate that the $\bar{\gamma}/\bar{A}$ ratio is, in fact, a function of the $\omega_{sp}/\omega_{knee}$ ratio, and they quantify Jones' claim that ω_{sp} should be much greater than ω_{knee}.

Fully Flexible Results

In performing the fully flexible analyses, a single configuration was used: the NASA DAST ARW-2 vehicle. This vehicle is a Firebee II target drone with its standard wings replaced with aeroelastic research wings. For these analyses, two rigid-body (plunge and pitch) and four symmetric flexible modes were used. The eigenvalues at the analysis condition of 0.7 Mach number and 15,000 ft altitude are plotted in Fig. 5. For this configuration, the short-period frequency is 21.7 times the knee frequency.

The PSD method and methods 1 and 2 of the SDG method were performed using the flexible-airplane equations of motion. For the PSD method, 1000 points were used in the numerical integration of Eq. (11). For the SDG method, the vehicles were each subjected to 50 single ramps.

Table 4 summarizes the PSD and SDG method 2 results. (Because of space limitations, only the method 2 results will be described). Because of the presence of flexible modes in the equations of motion, the resulting critical gust patterns are significantly more complicated than they were for the rigid-body analyses. Depending on the response, critical gust patterns are comprised of from three to ten single ramps. In addition, for half of the responses, the critical gust patterns

Table 5 Summary of statistical discrete gust-power spectral density comparisons

Type of analysis	Problem size	Computer resources: PSD CPU time (s)	PSD Field length	SDG CPU time (s)	SDG Field length	$\frac{\bar{\gamma}}{\bar{A}}$ Statistics: Mean	Standard deviation
Rigid-body (method 1)[a]	4	4	62 K	37	137 K	10.32	0.56
Fully flexible (method 1)[a]	52	134	170 K	2700	236 K	10.26	0.81
Fully flexible (method 2)[a]	52	134	170 K	4500	364 K	10.45	0.91

[a]Applies to SDG only.

contain overlapping ramps and subsequent ramps in the same direction.

As indicated in the last column of the table, all ratios of $\bar{\gamma}/\bar{A}$ fall between 8.45 (18.8% below 10.4) and 11.50 (10.6% above 10.4). The mean value of the ratios is 10.35 with a standard deviation of 0.96.

Figures 6 contain an example of the kind of time-correlated gust loads available from the SDG method. Figure 6a contains the critical gust pattern for mid bending moment as determined by method 2. It is comprised of three single ramps; the last two overlap each other and are in the same direction. Figure 6b contains the corresponding mid bending moment response with peak value occurring at about 1.4 s into the time history. Figure 6c contains the mid torsion-moment response resulting from the critical gust pattern for mid bending moment. Time histories of Figs. 6b and 6c are time-correlated gust loads.

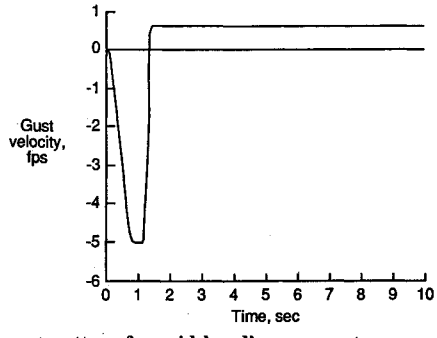

a) Critical gust pattern for mid bending moment.

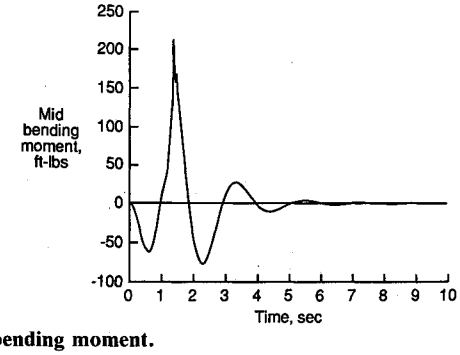

b) Mid bending moment.

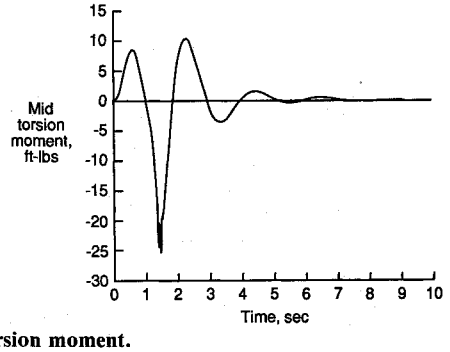

c) Mid torsion moment.

Fig. 6 Time-correlated gust loads from SDG method 2.

Observations

Table 5 contains a summary of the sizes of the problems solved, the computer resources required to solve those problems, and the statistics of the corresponding $\bar{\gamma}/\bar{A}$ ratios. Problem sizes have been expressed as the sum of the order of the linear system plus the number of outputs. All computer resources are for the NASA-Langley Control Data Corp. Cyber computers. The term computaional cost is defined to be the product of CPU time and field length. Several observations can be made:

1) For rigid-body and fully flexible analyses, the computational cost of performing an SDG analysis is significantly (20–30 times) larger than that of a PSD analysis.

2) The mean values of the $\bar{\gamma}/\bar{A}$ ratios remain within 2% of 10.4 for all implementations of the SDG method (methods 1 and 2).

3) The standard deviations of the $\bar{\gamma}/\bar{A}$ ratios about their respective means increase with the inclusion of flexible modes in the equations of motion.

Concluding Remarks

This paper has presented the results of a recent NASA investigation of the SDG-PSD overlap. SDG and PSD analyses were performed for several airplanes at different flight conditions, and responses from each method were compared to see if the 10.4 factor was obtained. Symmetric rigid-body analyses and symmetric fully flexible analyses were performed using linear equations of motion. In addition, an approximate form (method 1) and a more accurate form (method 2) of the SDG method were implemented and investigated.

During the investigation, several parameters were varied in an attempt to define quantitatively the limits of the overlap. Based on both the rigid-body and the fully flexible results, an SDG-PSD overlap does appear to exist. However, this overlap appears to be characterized, not by a 10.4 factor, but rather by a "10.4 plus-or-minus-approximately-five-percent factor" when rigid-body equations are involved, and by a "10.4 plus-or-minus-approximately-ten-percent factor" when fully flexible equations are involved.

Another significant finding was the relative computational costs of performing analyses using the PSD method and both SDG methods. An SDG method 1 analysis costs between 20 and 30 times as much as a PSD analysis; an SDG method 2 analysis costs twice that of an SDG method 1 analysis.

References

[1]Jones, J. G., "Statistical Discrete Gust Theory for Aircraft Loads," Royal Aircraft Establishment, Farnborough, Hampshire, England, TR 73167, 1983.

[2]Jones, J. G., "A Unified Procedure for Meeting Power-Spectral-

Density and Statistical-Discrete-Gust Requirements for Flight in Turbulence," AIAA Paper 86-1011, May 1986.

[3]Noback, R., "S.D.G., P.S.D. and the Nonlinear Airplane," National Aerospace Laboratory, Amsterdam, The Netherlands, NLR Rept. MP 88018 U, 1988.

[4]Jones, J. G., "On the Formulation of Gust-Load Requirements in Terms of the Statistical Discrete Gust Method," Royal Aircraft Establishment, Farnborough, Hampshire, England, TM FS 208, 1978.

[5]Jones, J. G., "Summary Notes on Statistical Discrete Gust Method," Royal Aircraft Establishment, Farnborough, Hampshire, England, TM FS 323, 1980.

[6]Jones, J. G., "An Equivalence Between Deterministic and Probabilistic Design Criteria for Linear Systems," *Journal of Sound and Vibration,* Vol. 125, No. 2, 1988, pp. 341–356.

[7]Jones, J. G., private communication, correspondence sent to the authors, 1988.

[8]Clementson, G. C., "An Investigation of the Power Spectral Density of Atmospheric Turbulence," Ph.D. Thesis, Massachusetts Institute of Technology, Cambridge, MA, 1950.

[9]Houbolt, J. C., Steiner, R., and Pratt, K. G., "Dynamic Response of Airplanes to Atmospheric Turbulence Including Flight Data on Input and Response," NASA TR-R-199, 1964.

[10]Hoblit, F. M., *Gust Loads on Aircraft: Concepts and Applications,* American Institute of Aeronautics and Astronautics, New York, 1988.

[11]Etkin, B., *Dynamics of Flight: Stability and Control,* Wiley, New York, 1959.

[12]Geising, J. P., Kalman, T. P., and Rodden, W. P., "Subsonic Unsteady Aerodynamics for General Configurations, Part I: Direct Application of the Nonplanar Doublet Lattice Method," Air Force Flight Dynamics Lab., Wright-Patterson AFB, OH, TR-71-5, 1971.

[13]Pototzky, A. S., and Perry, B., III, "New and Existing Techniques for Dynamic Loads Analysis of Flexible Airplanes," *Journal of Aircraft,* Vol. 23, No. 4, 1986, pp. 340–347.